

Inhibition of Monoamine Oxidases by Functionalized Coumarin Derivatives: Biological Activities, QSARs, and 3D-QSARs

Carmela Gnerre,[†] Marco Catto,[‡] Francesco Leonetti,[‡] Peter Weber,[†] Pierre-Alain Carrupt,[†] Cosimo Altomare,[‡] Angelo Carotti,[‡] and Bernard Testa^{*,†}

Institut de Chimie Thérapeutique, Université de Lausanne, BEP, CH-1015 Lausanne, Switzerland, and Dipartimento Farmaco-Chimico, University of Bari, I-70125 Bari, Italy

Received July 17, 2000

A large series of coumarin derivatives (71 compounds) were tested for their monoamine oxidase A and B (MAO-A and MAO-B) inhibitory activity. Most of the compounds acted preferentially on MAO-B with IC₅₀ values in the micromolar to low-nanomolar range; high inhibitory activities toward MAO-A were also measured for sulfonic acid esters. The most active compound was 7-[(3,4-difluorobenzyl)oxy]-3,4-dimethylcoumarin, with an IC₅₀ value toward MAO-B of 1.14 nM. A QSAR study of 7-X-benzylxy *meta*-substituted 3,4-dimethylcoumarin derivatives acting on MAO-B yielded good statistical results ($q^2 = 0.72$, $r^2 = 0.86$), revealing the importance of lipophilic interactions in modulating the inhibition and excluding any dependence on electronic properties. CoMFA was performed on two data sets of MAO-A and MAO-B inhibitors. The GOLPE procedure, with variable selection criteria, was applied to improve the predictivity of the models and to facilitate the graphical interpretation of results.

Introduction

Monoamine oxidase (MAO) is an FAD-containing enzyme tightly bound to the mitochondrial outer membrane of neuronal, glial, and other cells. Its roles include regulation of the levels of biogenic amines in the brain and the peripheral tissues by catalyzing their oxidative deamination.¹ On the basis of their substrate and inhibitor specificities, two types of MAO (A and B) have been described: MAO-A preferentially deaminates serotonin, norepinephrine, and epinephrine and is irreversibly inhibited by low concentrations of clorgyline; MAO-B preferentially deaminates β -phenylethylamine and benzylamine and is irreversibly inhibited by deprenyl.²

Due to their role in the metabolism of monoamine neurotransmitters, MAO-A and MAO-B present a considerable pharmacological interest. In Parkinson's disease (PD), dopamine (DA) replacement therapy with L-DOPA is the first-line treatment of this severe neurodegenerative disorder.³ Unfortunately, the rapid metabolic transformation of L-DOPA, at both the peripheral and central levels, strongly hampers its high therapeutic potential. For this reason, L-DOPA is typically combined with inhibitors of aromatic amino acid decarboxylase (AADC), such as benserazide and carbidopa, and/or with reversible and selective catechol *O*-methyltransferase (COMT) inhibitors, such as entacapone and tolcapone,⁴ and sometimes also with selective and irreversible MAO-B inhibitors, such as deprenyl.⁵

Paradoxically, recent findings indicate that both deprenyl and L-DOPA at high doses may induce neuronal apoptosis.⁶ In contrast, deprenyl at low doses exerts a significant neuroprotective effect by blocking apoptotic cell death.⁶ Interestingly, selective irreversible

MAO-A inhibitors, such as clorgyline, also seem to reduce neuronal cell death.⁷ Various observations stress the need for new, possibly reversible and safer MAO-B inhibitors in the therapy of PD and call for further investigations of the possible role of MAO-A inhibitors (already in use as antidepressants and antianxiety drugs⁸) as antiapoptotic agents in neurodegenerative diseases.

Unfortunately, the rational design of new MAO inhibitors (MAO-I) is strongly hampered by a lack of reliable three-dimensional structural information on the two active sites of the two isoenzymes. For this reason, several indirect modeling studies^{9–13} have been carried out on numerous and structurally diverse classes of MAO-I, but the molecular requirements responsible for selective MAO-A or MAO-B inhibition are only partly understood.

Coumarins are members of the class of compounds called benzopyrones and display a variety of pharmacological properties¹⁴ depending on their substitution pattern. Some coumarin derivatives of natural¹⁵ and synthetic origin¹⁶ have been characterized as MAO-I. To obtain a better understanding of the structure–activity relationships (SARs) of MAO-I and to improve their inhibitory activity, we have designed, prepared, and tested in vitro several 3-, 4-, 6-, and 7-substituted coumarins, as well as chromone derivatives and bicyclic compounds. Quantitative structure–activity relationships (QSARs) and 3D-QSAR models using the comparative molecular field analysis (CoMFA)/GOLPE approach are described in this paper. The results obtained reveal interesting features about the topography of the active site of MAO-A and MAO-B.

Results and Discussion

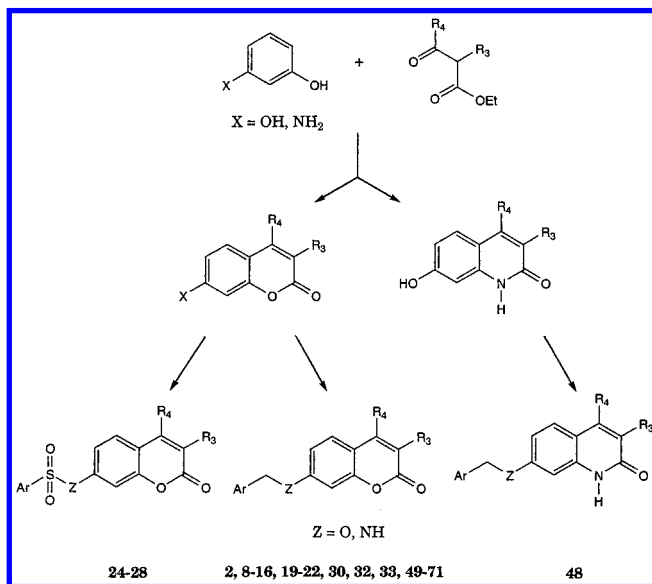
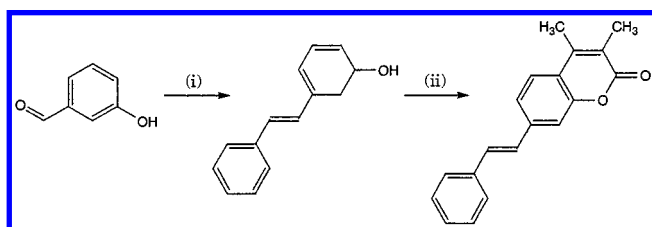
Chemistry. The structures of the compounds prepared in this study, mostly coumarin derivatives, are listed in Tables 1–4. Some of these compounds have

* To whom correspondence should be addressed. Phone: +4121 692 4521. Fax: +4121 692 4525. E-mail: Bernard.Testa@ict.unil.ch.

[†] Université de Lausanne.

[‡] University of Bari.

Scheme 1

Scheme 2^a

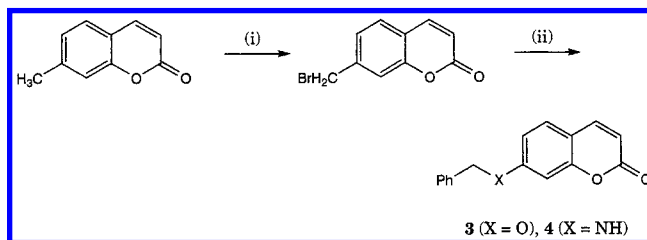
^a (i) Benzyl triphenylphosphonium chloride, Na, EtOH; (ii) ethyl 2-methylacetoacetate, H₂SO₄, 120 °C.

been patented^{17,18} and are already reported in the literature as reversible and selective MAO-I.¹⁶ The reaction yields and physicochemical and spectral data of the newly synthesized compounds are given in the Experimental Section and in Table S1 (Supporting Information).

The parent 7-hydroxycoumarins, if not commercially available, were prepared by the method of von Pechmann^{19,20} from *m*-resorcinol and the ethyl esters of appropriate β -keto acids, in the presence of catalytic amounts of sulfuric acid at 120 °C. The synthesis of 7-amino-3,4-dimethylcoumarin, the parent compound of **16**, **23**, and **28** (Table 1), was performed using ZnCl₂ in order to minimize the formation of the 7-hydroxyquinolin-2-one derivative. The latter was used as the starting material for the synthesis of compound **48** (Table 3). Hydroxy- or aminocoumarins were reacted with benzyl, benzoyl, or benzenesulfonyl halides under basic conditions to give the corresponding benzyl, benzoyl, or benzenesulfonyl derivatives. Scheme 1 illustrates the general pathway adopted for preparing most of the compounds examined in this study.

The 7-*trans*-styryl derivative **29** was prepared by reacting ethyl 2-methylacetoacetate with 3-*trans*-styrylphenol, the latter being prepared by a Wittig reaction using 3-hydroxybenzaldehyde and benzyltriphenylphosphonium chloride (Scheme 2).^{21,22}

Compound **9** was obtained by benzylation of 7-hydroxy-3,4-dihydrocoumarin, prepared by treating resorcinol and acrylic acid with Amberlist-15 in refluxing toluene, according to a known procedure,²³ whereas the

Scheme 3^a

^a (i) *N*-Bromosuccinimide, CCl₄, reflux; (ii) PhOH or PhNH₂, K₂CO₃, abs. EtOH, reflux.

starting material for the synthesis of compound **14** (i.e., 4,7-dihydroxycoumarin)²⁴ was easily prepared by the method of Dickenson²⁵ using 2,4-dihydroxyacetophenone and diethyl carbonate. Compound **21** was obtained by oxidizing **20** with DDQ.

7-Phenoxymethyl (**3**) and 7-anilinomethyl (**4**) coumarins were prepared by bromination of the methyl group of the commercial 7-methylcoumarin with *N*-bromosuccinimide (NBS) and subsequent nucleophilic displacement of bromide with phenol and aniline, respectively (Scheme 3).

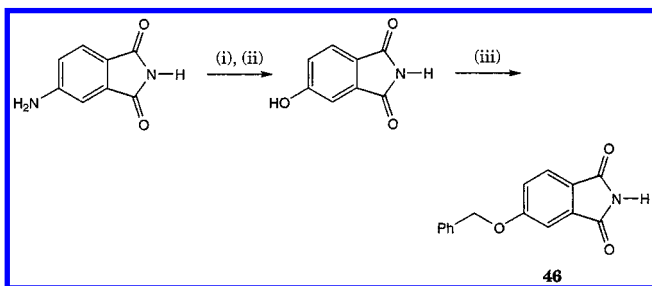
Compounds **30–32** were obtained through benzylation of 6,7-dihydroxy-3,4-dimethylcoumarin, the latter being prepared according to known procedures,²⁶ namely acetylation of *p*-benzoquinone to give 1,2,4-triacetoxybenzene and cyclization of this intermediate with ethyl 2-methylacetoacetate in 75% sulfuric acid.

The newly synthesized 7-X-substituted benzyloxy-3,4-dimethylcoumarins (i.e., **52**, **54–56**, **69–71**, see Table 4) were obtained by a classical alkylation reaction of 7-hydroxy-3,4-dimethylcoumarin with the appropriate benzyl bromide. The preparation of compounds **52** and **69** was carried out with the respective benzyl bromides, bearing the 3-OH groups protected as benzoyl esters. Reduction of the nitro group in compound **61** provided the amino congener **55**, and acetylation of **55** gave compound **56**.

According to reported procedures, the parent chromone derivatives (Table 2) were prepared from dihydroxyacetophenones by treatment with ethyl orthoformate and perchloric acid (**35** and **36**)²⁷ or alternatively by acylation, cyclization of the acyl intermediate in refluxing toluene in the presence of Na, and finally alkaline hydrolysis of the acyloxychromone derivative (**37–39**).²⁸ Compounds **36** and **37** are novel, and their physicochemical data are reported in Table S1 (Supporting Information).

The hetero-benzofused precursors of the compounds in Table 3 were prepared using previously reported procedures,^{29,30} whereas 5-benzyloxypthalimide was synthesized starting from the 5-amino congener in two steps: i.e., a diazotation/hydroxylation achieved via Sandmeyer reaction, by using Cu(NO₃)₂ and Cu₂O,³¹ and a subsequent classical alkylation of the OH group at the 5-position with benzyl bromide (Scheme 4). All other benzyloxy derivatives reported in Table 3 were prepared by a classical alkylation reaction of the hydroxy-substituted benzofused compounds.

MAO-A and MAO-B Inhibition. Seventy-one compounds, most of which are derivatives of 7-hydroxycoumarin, were tested for their inhibitory effect on MAO-A and MAO-B. To allow a separate analysis of their SARs, the compounds were divided into four series: namely a

Scheme 4^a

^a (i) NaNO₂, H₂O, H⁺; (ii) Cu(NO₃)₂, Cu₂O, H₂O; (iii) PhCH₂Br, K₂CO₃, abs. EtOH, reflux.

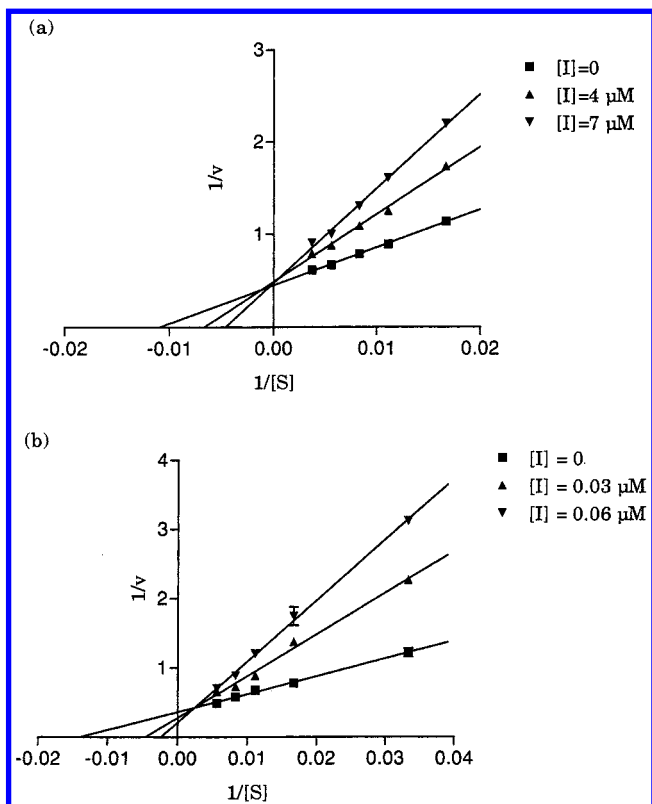


Figure 1. Lineweaver–Burk plots for compound **2** toward MAO-A (a) and MAO-B (b).

coumarin series (34 compounds, Table 1) with variations mainly in positions 3, 4, 6, and 7 of the coumarin nucleus, a second series (5 compounds, Table 2) grouping chromone derivatives, a third series (13 compounds, Table 3) with bicyclic structures containing a benzo moiety fused with various 5(or 6)-membered heterocycles, and a fourth series of 24 7-benzyloxy-substituted congeners of 3,4-dimethylcoumarin (Table 4) designed for QSAR purposes.

Lineweaver–Burk representations for compound **2** on MAO-A and MAO-B (Figure 1) demonstrate that its mechanism of inhibition was competitive in both cases. To confirm this mechanism for the other compounds, incubations were performed for all inhibitors at their IC₅₀, at a substrate concentration of 500 μM, resulting in a marked reduction in the calculated degree of inhibition. Preincubating the compounds for 15 instead of 5 min at their IC₅₀ and at the same substrate concentration did not affect the degree of inhibition.

MAO inhibition data expressed as pIC₅₀ values in Tables 1–4 show that the majority of the compounds

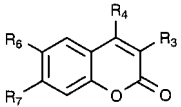
act preferentially as MAO-B inhibitors, with IC₅₀ values in the micromolar to low-nanomolar range. From a SAR viewpoint, it appears that substitution at the 7-position of the coumarin nucleus is essential for good inhibitory activity.

The most active MAO-B inhibitor was 7-[(3,4-difluorobenzyl)oxy]-3,4-dimethylcoumarin (**67**; Table 4) with an IC₅₀ value of 1.14 nM, whereas the most active MAO-A inhibitor was 7-(4-nitrophenylsulfonyloxy)-3,4-dimethylcoumarin (**27**; Table 1) with an IC₅₀ value of 10.7 nM. These experimental observations agree with previous literature data¹⁶ demonstrating a key role of the 7-substituent, the ether derivatives being MAO-B selective but the sulfonic acid esters displaying MAO-A selectivity. It is worth noting that for compounds **15** and **62–64**, we observed the same activity rank order as reported in the literature (i.e., **62** < **15** < **63** ≈ **64**).¹⁶ Typically, our data, determined by a different method (spectrophotometric versus radiochemical assay), showed pIC₅₀ values lower by up to 1 order of magnitude compared to those reported by Rendenbach-Müller et al.¹⁶

Qualitative SARs. For MAO-B inhibition, a comparison between the biological data of the coumarin derivatives in Table 1 and the compounds in Tables 2 and 3 unequivocally proved the essential role of the coumarin nucleus. In fact, compared with the MAO-B inhibitory activity of the coumarins (Tables 1 and 4), the chromone derivatives **35–39**, the 2-quinolinone derivative **48**, and all other bicyclic compounds containing a benzofused 5-membered heterocycle showed lower MAO-B inhibition, the most active inhibitor **37** having a pIC₅₀ value of 6.90.

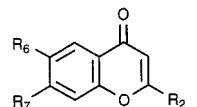
Within the coumarin series (Table 1), 7-benzyloxy-coumarin (**2**) was quite active and selective toward MAO-B. Hydrogenation of the 3,4-double bond (**9**), as well as a substituent in the 6-position regardless of size and lipophilicity (**5–8**), abolished or significantly decreased activity. Substitution at positions 3 and/or 4 of the coumarin nucleus modulated MAO-B inhibitory activity and A/B selectivity. Indeed, monosubstitution in position 4 with a CH₃ led to more active compounds (**10** and **11**), whereas phenyl (**12**), trifluoromethyl (**13**), and hydroxy (**14**) groups at the same position decreased activity. Simultaneous substitution with methyl groups at positions 3 and 4 was even more favorable for MAO-B inhibition activity (compare **15** with **2** and **10**). 3,4-Annellation with 5- and 6-membered rings was favorable only for the cycloaliphatic and smaller cyclopentenyl rings (compare **19** with **15**, **20** and **21**). The coumarin derivative **22** bearing phenyl and methyl groups at positions 3 and 4, respectively, lacked both MAO-A and MAO-B inhibitory activity. From such a rank order of activity, we can infer that the MAO-B binding site should accept lipophilic substituents of limited size at positions 3 and 4 of the coumarin nucleus, whereas hydrophilic (e.g., OH) or larger hydrophobic (e.g., CF₃, phenyl) are not well tolerated. Other factors of electronic nature may interfere in the case of CF₃ substituent.

As for the structural variations of substituents at the 7-position, it appears that the benzyloxy substituent elicits ideal interactions within the MAO-B binding pocket. In fact, a simple inversion of the direction of the OCH₂ functionality (**2** versus **3**) leads to a slight

Table 1. Chemical Structures and MAO Inhibition Data of Coumarin Derivatives


compd	R ₃	R ₄	R ₆	R ₇	pIC ₅₀ ^a	
					MAO-A	MAO-B
1	H	H	H	H	4.39	4.92
2	H	H	H	OCH ₂ C ₆ H ₅	5.17	7.26
3	H	H	H	CH ₂ OC ₆ H ₅	6.41	7.07
4	H	H	H	CH ₂ NHC ₆ H ₅	4.38	5.67
5	H	H	OCH ₃	OCH ₂ C ₆ H ₅	18% (50 μM)	5.17
6	H	H	OCH ₂ C ₆ H ₅	OH	4.63	5.69
7^b	H	H	glucosyl	OH	9% (100 μM)	7% (100 μM)
8	H	H	glucosyl	OCH ₂ C ₆ H ₅	15% (100 μM)	11% (100 μM)
9^c	H ₂	H ₂	H	OCH ₂ C ₆ H ₅	4 μM ^d	20% (4 μM)
10	H	CH ₃	H	OCH ₂ C ₆ H ₅	5.71	7.74
11	H	CH ₃	H	OCH ₂ C ₆ H ₄ -3'-NO ₂	6.90	7.88
12	H	C ₆ H ₅	H	OCH ₂ C ₆ H ₅	4 μM ^d	4 μM ^d
13	H	CF ₃	H	OCH ₂ C ₆ H ₅	5 μM ^d	5.86
14	H	OH	H	OCH ₂ C ₆ H ₅	26% (15 μM)	5.80
15	CH ₃	CH ₃	H	OCH ₂ C ₆ H ₅	6.16	8.36
16	CH ₃	CH ₃	H	NHCH ₂ C ₆ H ₅	5.80	6.79
17	CH ₃	CH ₃	H	O(CH ₂) ₂ C ₆ H ₅	6.00	8.25
18	CH ₃	CH ₃	H	OCH(CH ₃)C ₆ H ₅	5.45	6.49
19	(CH ₂) ₃		H	OCH ₂ C ₆ H ₅	5.80	8.46
20	(CH ₂) ₄		H	OCH ₂ C ₆ H ₅	5.80	8.46
21	(-CH=CH-) ₂		H	OCH ₂ C ₆ H ₅	7% (1 μM)	7.30
22	C ₆ H ₅	CH ₃	H	OCH ₂ C ₆ H ₅	4% (3 μM)	8% (3 μM)
23	CH ₃	CH ₃	H	NHCOC ₆ H ₅	5.86	6.72
24	CH ₃	CH ₃	H	OSO ₂ C ₆ H ₅	7.12	5.28
25	CH ₃	CH ₃	H	OSO ₂ C ₆ H ₄ -4'-CH ₃	7.33	17% (15 μM)
26	CH ₃	CH ₃	H	OSO ₂ C ₆ H ₄ -4'-OCH ₃	7.15	4.77
27	CH ₃	CH ₃	H	OSO ₂ C ₆ H ₄ -4'-NO ₂	7.90	20% (2 μM)
28	CH ₃	CH ₃	H	NHSO ₂ C ₆ H ₄ -4'-CH ₃	4.17	29% (40 μM)
29	CH ₃	CH ₃	H	<i>trans</i> -CH=CHC ₆ H ₅	6.39	7.55
30	CH ₃	CH ₃	OH	OCH ₂ C ₆ H ₅	5.03	7.55
31	CH ₃	CH ₃	OCH ₂ C ₆ H ₅	OH	3.95	5.51
32	CH ₃	CH ₃	OCH ₂ C ₆ H ₅	OCH ₂ C ₆ H ₅	0.4 μM ^d	0.4 μM ^d
33^e	CH ₃	CH ₃	H	OCH ₂ C ₆ H ₅	6.25	5.48
34^f	CH ₃	CH ₃	H	OH	35% (30 μM)	18% (30 μM)

^a Or percent inhibition at maximum solubility in parentheses; SD on IC₅₀ values < 10%. ^b Esculin (natural product). ^c 3,4-Dihydrocoumarin derivative. ^d No inhibition at maximum solubility. ^e 8-Methyl derivative. ^f 5-OCH₂C₆H₅ derivative.

Table 2. Chemical Structures and MAO Inhibition Data of Chromone Derivatives


compd	R ₂	R ₆	R ₇	pIC ₅₀ ^a	
				MAO-A	MAO-B
35	H	H	OCH ₂ C ₆ H ₅	4.79	5.98
36	H	OCH ₂ C ₆ H ₅	H	5.17	6.25
37	CH ₃	OCH ₂ C ₆ H ₅	H	4.66	6.90
38	C ₆ H ₅	H	OCH ₂ C ₆ H ₅	6% (1 μM)	6% (1 μM)
39	C ₆ H ₅	OCH ₂ C ₆ H ₅	H	3 μM ^b	38% (3 μM)

^a Or percent inhibition at maximum solubility in parentheses; SD on IC₅₀ values < 10%. ^b No inhibition at maximum solubility: 3 μM.

decrease in MAO-B and a significant increase in MAO-A inhibitory activity. As a result, a strong drop of B/A selectivity was observed. Increasing the length of the ether bridge with a further methylene group did not significantly change activity (**15** versus **17**). The comparison of the activity values of compounds **30–32**, as well as the activity of derivatives **5–7** and the natural product esculin (**8**), clearly reveals the effect of steric hindrance at position 6: only small substituents such as OH are tolerated, even though both MAO-A and MAO-B activities decreased by about 1 order of mag-

nitude (**15** versus **30**). The CH₂NH bridge at the 7-position (**16**) decreased both MAO-A and MAO-B inhibition, the latter much more than the former. The inverted NHCH₂ bridge (compound **4**) produced similar effects. MAO inhibition effects were maintained from a NHCH₂ (**16**) to a NHCO (**23**) bridge.

Due to its good MAO-B activity and selectivity, derivative **15** was taken as a lead compound to explore SARs by various substitutions of the phenyl ring of the 7-benzyloxy group in the 2-, 3-, and 4- positions (Table 4). Derivatives bearing halogen substituents (**57**, **58**, **63**, **64**, **67**, **68**), are more active than compound **15** toward MAO-B. In two cases when a comparison between positional isomers was possible (CH₃ and CN congeners), *ortho*-substitution appeared unfavorable. Among the *para*-substituents, halogens (**63** and **64**) elicited the highest activities. The compounds in Table 4 were also active toward MAO-A, their degree of B/A selectivity ranging from about 3 (**51**) to about 1 (**69**) log units. However, the congeners showing MAO-A inhibitory activity higher than (or close to) that of the lead **15** are the ones bearing strong electron-withdrawing substituents (NO₂, CN) irrespective of their position (**50**, **60**, **61**, **65**, **66**, **70**) or a halogen in the *para*-position (**63**, **64**, **67**, **69**). The role of steric hindrance in influencing MAO-A inhibition is suggested by the strong decrease in activity of the congeners bearing bulkier substituents

Table 3. Chemical Structures and MAO Inhibition Data of Hetero-Benzofused Derivatives Bearing a Benzyloxy Substituent

compd	C	pIC ₅₀ ^a	
		MAO-A	MAO-B
40		0% (8 μM)	5.59
41		4.40	6.30
42		30% (50 μM)	5.74
43		5.44	6.63
44		0% (20 μM)	4.23
45		18% (30 μM)	5.62
46		25% (5 μM)	6.41
47		3.99	5.98
48		0% (2 μM)	6.20

^a Or percent inhibition at maximum solubility in parentheses; SD on IC₅₀ values < 10%.

(e.g., **54** and **56**). These preliminary considerations bring useful information on the main physicochemical properties modulating selectivity toward the two isoforms of MAO.

It had previously been reported¹⁶ that the selectivity of coumarin inhibitors was reversed by an O-SO₂ function. Our data confirm this observation (compare compounds **24–27** with **15** and its congeners). Interestingly, the introduction of the isosteric NHSO₂ group (compound **28**) canceled both MAO inhibitory activities, likely due the ionizable group (pK_a = 7.05 in 5% DMSO/water). Unfavorable steric effects resulted from the introduction of a CH₃ group on the oxymethylene bridge, as already shown.¹⁶ Indeed, with compound **18** a marked drop in MAO-B activity relative to compound **15** was observed whereas MAO-A inhibition was only slightly decreased. From a structure–selectivity relationship viewpoint, another interesting comparison can be made between the inhibitory activity of compounds **15** and **33**, since the introduction of a methyl group at the 8-position in compound **15** dramatically inverted selectivity toward MAO-A (ΔpIC₅₀ ranges from 2.20 in compound **15** to –0.77 in compound **33**). This appears due mainly to a drop in MAO-B inhibition of about 3 orders of magnitude (from 8.24 to 5.48), the MAO-A inhibitory activity remaining almost constant. Another structural factor enhancing MAO-B selectivity appears to be the introduction in compound **2** of methyl groups (**15**) or a fused cyclopentenyl ring (**19**) at positions 3 and 4 of the

Table 4. MAO Inhibition Data and Physicochemical Parameters Used for the QSAR Study of 7-X-Substituted Benzyloxy-3,4-dimethylcoumarins

compd	X	pIC ₅₀ ^a		π	V _w	F
		MAO-A	MAO-B			
15	H	6.16	8.36	0	0.08	0
49	2-CH ₃	5.64	8.06	0.44	1.01	–0.05
50	2-CN	6.38	7.64	–0.43	1.14	0.64
51	3-CH ₃	5.48	8.36	0.49	1.01	–0.04
52	3-OH	6.38	8.01	–0.67	0.49	0.28
53	3-OCH ₃	5.82	8.44	–0.09	1.49	0.25
54	3-OCF ₃	5.23	7.94	1.02	1.60	0.37
55	3-NH ₂	6.00	7.46	–1.23	0.67	0.02
56	3-NHCOCH ₃	5.15	6.60	–0.99	2.70	0.27
57	3-F	6.24	8.55	0.14	0.36	0.42
58	3-Cl	5.95	8.48	0.71	1.07	0.40
59	3-CF ₃	5.72	8.24	0.88	1.11	0.37
60	3-CN	6.66	7.97	–0.57	1.14	0.50
61	3-NO ₂	7.12	8.59	–0.26	1.20	0.66
62	4-CH ₃	5.43	8.21	0.49	1.01	–0.04
63	4-F	6.91	8.52	0.14	0.36	0.43
64	4-Cl	6.91	8.59	0.71	1.07	0.41
65	4-CN	7.00	8.43	–0.57	1.14	0.51
66	4-NO ₂	6.08	8.07	–0.26	1.20	0.67
67	3,4-F ₂	6.91	8.94	0.21	0.72	0.85
68	3,5-F ₂	6.17	8.52	0.28	0.72	0.84
69	3-OH, 4-F	6.94	8.13	–0.43	0.85	0.71
70	3,5-(NO ₂) ₂	6.74	8.19	–0.52	2.40	1.32
71	pentafluoro	6.16	8.23	0.57	1.80	2.35

^a SD on IC₅₀ values < 10%.

coumarin nucleus. In contrast, changing the benzyloxy substituent at position 7 of compound **2** (ΔpIC₅₀ = 2.09) with other groups generally resulted in a significant decline in MAO-B selectivity (see, for example, compounds **3** and **4**), the higher effect being observed for the 7-phenoxyethyl derivative **3**.

QSAR Study of 7-X-Benzyloxy-Substituted 3,4-Dimethylcoumarin Congeners. To understand the relationship between their MAO inhibitory activity and physicochemical properties, a Hansch-type QSAR study of the 24 substituted congeners of 7-X-benzyloxy-3,4-dimethylcoumarin (Table 4) was carried out by stepwise multiple linear regression (MLR) with cross-validation. Each substituent was described by six parameters. The Hansch constant (π), calculated from CLOGP values,³² was used as a descriptor of lipophilicity, bulkiness was parametrized by the van der Waals volume (V_w) and molar refractivity (MR), taken from standard compilations,^{33–35} whereas classical Hammett (σ_m and σ_p) and Swain–Lupton (F and R) constants were used as electronic parameters. The F and R parameters for the substituents at the *meta*- and *ortho*-positions were corrected according to Williams and Norrington.³⁶

The squared correlation matrix of variables used in MLR is reported in Table 5. MAO-A and MAO-B inhibitory activity values (pIC₅₀) are poorly correlated, indicating that the same physicochemical properties modulate differently the inhibition of the two MAO isoforms.

Taking into account our previous QSAR results with pyridazines as reversible MAO-B inhibitors,^{37,38} we first examined the relation between lipophilicity and pIC₅₀

Table 5. Squared Correlation Matrix of Parameters Used in QSAR (values in Table 4)^a

	pIC ₅₀ (A)	pIC ₅₀ (B)	ΔpIC ₅₀	π	V _w	F
pIC ₅₀ (A)	1	0.243 (0.230)	0.441 (0.266)	0.075 (0.086)	0.081 (0.263)	0.132 (0.231)
pIC ₅₀ (B)		1	0.104 (0.255)	0.280 (0.337)	0.250 (0.373)	0.026 (0.045)
ΔpIC ₅₀			1	0.565 (0.732)	0.014 (0.009)	0.066 (0.070)
π				1	0.015 (0.005)	0.003 (0.019)
V _w					1	0.143 (0.060)
F						1

^a In parantheses, squared correlation matrix relative to the subset of *meta*-X-substituted congeners.

values. Cross-validated MLR carried out on the whole set of congeners did not yield statistically significant equations, although an inspection of the plot (see below) of MAO-B inhibition data against π values suggested a nonlinear (likely parabolic) relationship. A quadratic regression performed on all the 24 congeners afforded an equation explaining less than 60% of the variance in the biological data and having a cross-validation parameter too low to be considered predictive ($q^2 = 0.25$). In contrast, performing regression analysis on the subset of the *meta*-X-monosubstituted derivatives, whose substituents explore a larger space than the *para*-derivatives in terms of lipophilic, steric, and electronic properties, afforded more quantitative information on the physicochemical properties governing inhibition. Indeed, by omitting only the *meta*-acetamido congener **56** as the strongest outlier, we obtained the following parabolic equation for the *meta*-isomers:

$$\text{pIC}_{50}(\text{MAO-B}) = 0.19(\pm 0.15)\pi - 0.56(\pm 0.21)\pi^2 + 8.46(\pm 0.14) \quad (1)$$

$$n = 11; r^2 = 0.86; q^2 = 0.72; s = 0.14; F = 24.13$$

where n represents the numbers of data points, r^2 the squared correlation coefficient, q^2 the leave-one-out cross-validation coefficient, and s the standard deviation of the regression equation; 95% confidence intervals of the regression coefficients are given in parentheses. Equation 1 explains more than 85% of the variance in the inhibition data and has a satisfactory predictive ability. The parabolic eq 1 is graphically illustrated in Figure 2, where the data of the other positional isomers have been added for comparison.

Figure 2 suggests that most of the 7-X-benzyloxy-3,4-dimethylcoumarin congeners follow quite well the parabolic relationship described by eq 1. Three compounds, namely the two *ortho*-substituted derivatives **49** (X = 2-CH₃) and **50** (X = 2-CN) and the *meta*-NHCOCH₃ congener **56**, deviated strongly from the regression curve, suggesting that other factors, presumably steric and/or conformational, are not accounted for by the quadratic equation. We believe that the deviating behavior of compound **56** could be ascribed to the large size of its *meta*-acetamido substituent (whose van der Waals volume equals 2.70, a value significantly higher than those of the other substituents, ranging between 0.08 and 1.49), whereas cyano and methyl substituents at the *ortho*-position of the phenyl ring may produce

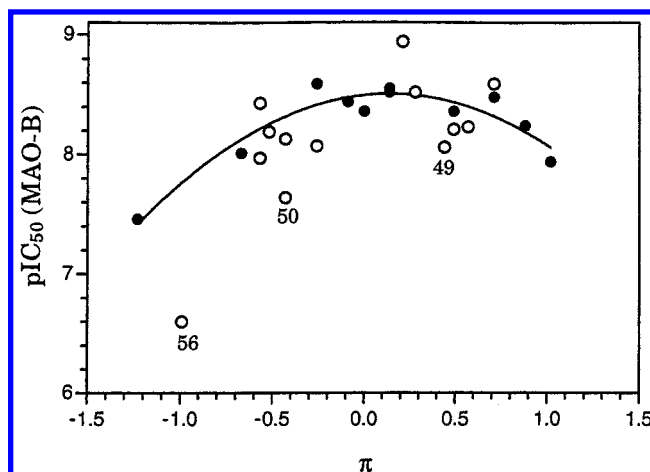


Figure 2. Plot of pIC₅₀ (MAO-B) values versus Hansch hydrophobic constant π. The parabolic curve is a graphical representation of eq 1. Filled circles represent the data set ($n = 11$) generating eq 1, whereas unfilled circles represent the other congeners of Table 4.

steric hindrance unfavorable to the interaction of compounds **49** and **50** with the binding site. Apparently, electronic factors should not play an important role, since incorporating any electronic constant into regression models did not result in equations better than eq 1.

Within the limits of the examined property space, it can be inferred that cooperative lipophilic interactions of *meta*-X substituents play the most important role in modulating MAO-B inhibition, with an optimum value of π around 0.2. Besides lipophilicity, a proper steric fit of the *meta*-substituents may be hypothesized, whereas QSAR analysis clearly excluded a dependence on electronic properties.

With the lipophilicity parameter alone, no significant result was obtained for MAO-A inhibition, whereas a trend between electronic, steric, and lipophilic features and MAO-A inhibition was detected within the subset of *meta*-X-substituted 7-benzyloxy coumarins. A three-parameter equation having satisfactory fitting (but not cross-validated) statistics ($r^2 = 0.85$, $q^2 = 0.56$) was obtained, which suggests favorable effects of electron-withdrawing and less bulky substituents and a minor and negative effect of lipophilicity.

The number of *para*- and *ortho*-X-substituted congeners synthesized and tested so far and the property space examined with them are too limited to allow a systematic comparison between positional isomers. Nevertheless, the above QSAR results, although limited to the *meta* subset, suggest that the MAO-B binding site (eq 1) should be different from that of MAO-A in terms of hydrophobic and polar properties.

As far as selectivity is concerned, the regression analysis performed on the difference between MAO-B and MAO-A inhibition ($\Delta\text{pIC}_{50} = \text{pIC}_{50}(\text{MAO-B}) - \text{pIC}_{50}(\text{MAO-A})$) gave the following equation for the *meta*-congeners:

$$\Delta\text{pIC}_{50} = 0.72(\pm 0.21)\pi - 1.08(\pm 0.72)F + 2.44(\pm 0.26) \quad (2)$$

$$n = 12; r^2 = 0.88; q^2 = 0.83; s = 0.22; F = 33.28$$

Table 6. Statistical Results for Data Sets A, A1, B, and B1 with Steric (ste), Molecular Electrostatic Potential (mep), and Lipophilic (lip) Fields

SAMPLS Results (q^2)								
data set	<i>N</i>	ste	mep	lip	ste and mep	ste and lip	mep and lip	ste, mep, and lip
A	2	0.14	0.39	0.17	0.44	0.28	0.43	0.45
A1	2	<0	0.52	0.17	0.46	0.05	0.56	0.53
B	2	0.15	0.27	0.42	0.43	0.45	0.51	0.52
B1	2	0.30	0.65	0.44	0.67	0.55	0.66	0.70
Final models after variable selection								
data set		fields	variables	<i>N</i>	q^2	r^2		
A1		mep	290	2	0.58	0.68		
B1		ste, mep, and lip	355	2	0.80	0.88		

explaining 88% of the variance in the selectivity data with a good cross-validation result. Attempts to extend the regression model to the whole set of congeners resulted in statistically poor equations, most likely because of the limited physicochemical property space explored by congeners different from the *meta*-substituted ones. However, within the limits of the examined structural space, eq 2 shows that 7-*X*-benzyloxy-3,4-dimethylcoumarins bearing lipophilic and electron-donating (field effect) substituents at the *meta*-position inhibited MAO-B better than MAO-A. Taken globally, eqs 1 and 2 indicated lipophilicity as the property that should influence MAO-B versus MAO-A selectivity, whereas the presence of an electron-withdrawing substituent should favor MAO-A inhibition.

These findings agree with our previous QSAR results obtained with a large series of structurally diverse reversible MAO-I, i.e., 5*H*-indeno[1,2-*c*]pyridazine derivatives,³⁷ where we also demonstrated lipophilic interactions to play a significant role in increasing MAO-B selectivity. However, most of the pyridazine MAO-I elicited measurable activity only toward the B form, and this prevented us from obtaining detailed and quantitative information on other physicochemical properties modulating selectivity. In contrast, the coumarins, especially the 7-benzyloxy-3,4-dimethylcoumarin derivatives (Table 4) reported herein, were very good inhibitors of MAO-B with sometimes appreciable activities toward the A isoform. This allowed us to accurately assess A/B selectivity and also to carry out multiple regression analysis providing helpful information to design inhibitors. Indeed, lipophilicity proved again to be a major property favoring the binding of coumarins to MAO-B, whereas a π -electron-poor phenyl ring in the 7-position appears to improve both MAO-A and MAO-B inhibition, leading to more active but slightly less selective inhibitors.

3D-QSAR Study of MAO Inhibition. CoMFA, a very useful tool in 3D-QSARs,³⁹ was used to analyze the numerous biological data obtained for MAO-A and MAO-B inhibition. The need to validate and better interpret the results generated with the classical CoMFA procedure of SYBYL prompted us to use GOLPE. Training sets of 41 coumarin derivatives acting as MAO-A inhibitors (set A) and 44 as MAO-B inhibitors (set B) were chosen among the numerous compounds available using the following criteria: only the inhibitors containing a coumarin ring and substituted in the 3-, 4-, or 7-position were selected, to have a good variability in substituents. The experimental activities were expressed as the negative logarithm of IC₅₀ (M) (pIC₅₀).

Alignment is considered to be a crucial step in every CoMFA study. The compounds investigated here present a relatively flexible substituent in position 7. Their conformational behavior was calculated with the MMFF94s⁴⁰ force field, and the conformation chosen was a flat one with a maximal energy of 4 kcal/mol above the minimum. The molecules were then superimposed on the coumarin ring, and a regularly spaced (1.5 Å) 3D grid was used.

First, SAMPLS analysis, with steric field, molecular electrostatic potential, and molecular lipophilicity potential, was run in SYBYL for sets A and B to determine which fields were statistically significant. Then, the CoMFA columns were exported in GOLPE where a PCA was performed on the *X*-variables matrix and the first three components were used to observe the objects (molecules) in the space of the principal components (PCs). PLS analysis was then applied and a PLS plot representing the objects in the space of *X*-scores (*T*) against *Y*-scores (*U*) was examined. PCA score plots together with the PLS plot allowed the identification of outliers, which were removed in the final analysis.

The *X*-variables of each set were submitted, in GOLPE, to an advanced pretreatment and then grouped using the smart region definition (SRD) algorithm. Finally a variable selection (fractional factorial design, FFD) was applied in order to retain only the informative variables. The details of the parameters used in each step are given in the Experimental Section.

3D-QSAR of MAO-A Inhibitors. The results for SAMPLS analysis on data set A are presented in Table 6. The cross-validation values for this data set are relatively small and would be considered insignificant were it not for the possibility to use GOLPE. The only field that could explain MAO-A activity is the electrostatic one. This field was exported in GOLPE, and a PCA was applied in order to observe the position of the objects. The first component revealed clearly that compounds **1** and **4**, which have a relatively weak activity, are not well discriminated in relation to the other objects of the set. After a PLS analysis, the viewing of the PLS plot on the first component confirmed that these two compounds are outliers. Compound **1** has a smaller size than all other molecules in the data set and this can be an explanation. For compound **4**, the conversion of the oxymethylene bridge to a methyleneamino led to a significant loss in activity which could not be explained by the model. Compounds **1** and **4** were removed from data set A; the cross-validation results for the SAMPLS analysis applied to the new data set A1 are also presented in Table 6. The

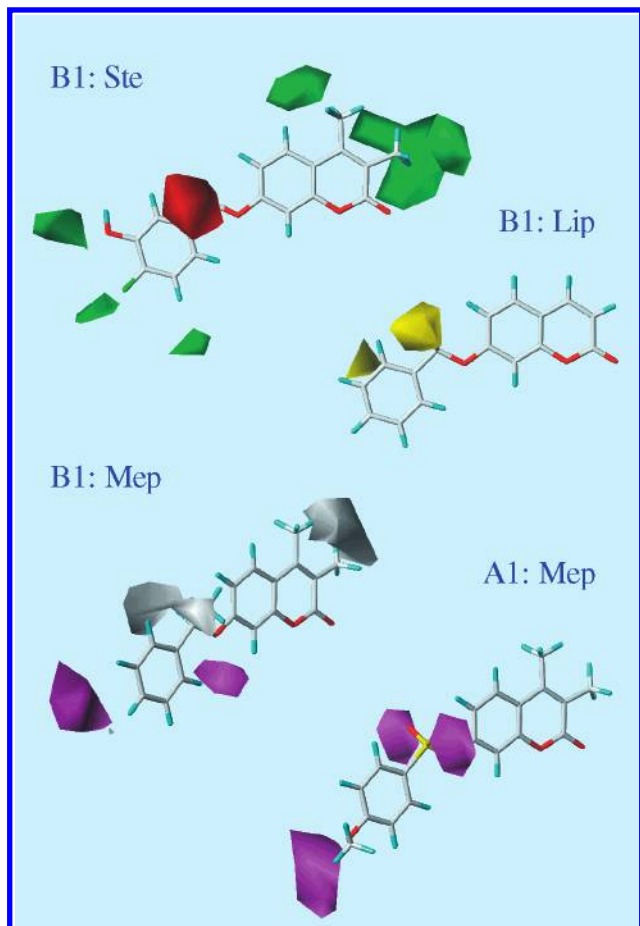


Figure 3. Statistical fields of 3D-QSAR models for MAO-A and MAO-B inhibition, obtained after variable selection in GOLPE: PLS coefficients. The color codes are the following: sterically favorable and unfavorable influences, green and red zones, respectively; favorable influence of lipophilic groups, yellow zone; favorable influence of high electron density and deficiency, magenta and white zones, respectively. (B1) Results of the model for MAO-B inhibitors (actual values of PLS coefficients: ste, 0.0016/−0.0016; lip, 0.0025; mep, 0.0016/−0.0017). Substitution at positions 3 and 4 of the coumarin ring have a favorable steric contribution, whereas substitution in the lateral chain is sterically unfavorable. The substitution of positions 3, 4, and 5 in the phenyl ring of the benzyloxy is also sterically favorable but in a less important manner. The lipophilic character of the CH₂ position in the oxymethylene bridge is favorable for activity. The magenta zones near the 7-position of the coumarin ring indicate that a high electron density is favorable for activity. Electron-withdrawing substituents at the 3- and 4-positions in the benzyloxy ring produce favorable zones for activity. Electron deficiency in positions 3 and 4 of the coumarin ring and near the 7-position on the oxymethylene bridge is favorable for the activity. (A1) Results of the model for MAO-A inhibitors (actual values: mep, −0.0015). Two electron-rich zones around the oxymethylene bridge clearly indicate a favorable influence on activity, as well as another one in the 4-position on the benzyloxy ring.

model with the MEP field built with data set A1 is the only one able to explain the MAO-A activity. Variable selection, whose parameters can be found in the Experimental Section, leads to a slightly improved cross-validation coefficient, also obtained with a “leave-one-out” procedure (Table 6), and a clearer representation of the contour maps.

Indeed, graphical results represented in Figure 3 (A1) show that there are two electron-rich favorable zones in the lateral chain. These zones are due to the presence

of the sulfone in the most active compounds (**24–27**). The third magenta zone in the *para*-position of the phenyl ring indicates the favorable effect of electron-withdrawing substituents on MAO-A activity.

3D-QSAR of MAO-B Inhibitors. The results for the SAMPLS analysis on data set B are presented in Table 6. The three fields were exported in GOLPE in order to observe the objects after a PCA carried out on each field separately and then in combination. A PLS was also applied to observe the PLS plot on the first component. In this case two outliers were identified, namely compounds **3** and **23**. These two compounds, again, present structural modifications of the benzyloxy in position 7, leading to differences in activity which cannot be explained by the model. They were removed from set B, and the results of the SAMPLS analysis are in Table 6. The cross-validation coefficients are significantly improved by the removal of these two outliers. A model with the combination of the three fields was chosen and submitted to a variable selection (see Experimental Section for details). The graphical results obtained after variable selection are presented in Figure 3 (B1). Sterically favorable green zones are present at positions 3 and in a lesser extent 4 of the coumarin ring, because compounds substituted in position 4 do not always show a better MAO-B inhibitory activity (e.g., compounds **13** and **14**). The other sterically favorable zones on the phenyl ring are due to the presence of substituents increasing activity, such as chloro, cyano, and methoxy. Concerning the lipophilic field, it seems that the presence of a favorable yellow zone on the lateral chain is correlated with the information given by the MEP field: there is a favorable electron-deficient white zone in the same position. There is another electron-deficiency zone in the coumarin ring generated by substituents such as a fused cyclopentenyl or cyclohexenyl ring which enhances activity but also generated by substituents such as OH which decrease it. Two other electron-rich favorable zones are present: one on the lateral chain near the oxygen of the oxymethylene bridge in position 7 and the other between the *para*- and *meta*-positions of the phenyl ring.

Conclusion

Coumarin derivatives proved to be competitive and reversible MAO-I, usually with a high selectivity for MAO-B. The most potent compound (**67**) has an IC₅₀ = 1.14 nM. However, a very potent MAO-A inhibitor (**27**) was also found (IC₅₀ = 10.7 nM).

Taken together, the results from our QSAR and CoMFA/GOLPE studies afford coherent information about the nature and spatial location of the main interactions underlying the potency and selectivity of MAO-I. The main features required for selectivity are the lipophilic character of substituents on the phenyl ring increasing MAO-B selectivity and the presence of a sulfonic ester function at position 7 leading to a higher MAO-A activity and suggesting the presence of a hydrophilic, polar pocket in the active site of the isoenzyme.

As observed in several previous studies, the coordinated application of 2D- and 3D-QSAR methods yields significant and complementary insights into SARs, offering at the three-dimensional level a clear picture

of the main forces modulating chemical and biological processes.⁴¹

Our findings are in good agreement with previous SAR studies on MAO-I. Being based on a rather large array of compounds properly designed for a QSAR study and on a homogeneous data set spanning quite regularly a wide range of inhibitory activity, they can be judiciously used for the design of new potent and selective MAO-I.

Experimental Section

Chemistry. Melting points were determined by the capillary method on a Gallenkamp MFB 595 010M electrothermal apparatus and are uncorrected. Elemental analyses were performed on a Carlo Erba 1106 analyzer for C, H, and N. The results agreed within $\pm 0.40\%$ of the theoretical values. IR spectra were recorded using a potassium bromide disk on a Perkin-Elmer 1600 FT-IR spectrophotometer. Only the most significant IR absorption bands are listed in Table S1 (Supporting Information). ¹H NMR spectra were recorded at 300 MHz on a Bruker 300 instrument. Chemical shifts are expressed in δ (ppm) and the coupling constants J in hertz (Hz). The following abbreviations are used: s, singlet; d, doublet; t, triplet; dd, double doublet; dq, double quadruplet; td, triple doublet; tt, triple triplet; m, multiplet; br, broad signal. Signals due to OH and NH protons were located by deuterium exchange with D₂O.

Chromatographic separations were performed on silica gel (230–400 mesh, Merck) using the flash methodology. Starting materials, unless otherwise stated, are commercially available and were purchased from Sigma-Aldrich (Milano, Italy). Several compounds were synthesized according to reported procedures with slight modifications; melting points and spectral data were in full agreement with those reported in the literature.

General Procedure for the Synthesis of Coumarin Derivatives. When not commercially available, 7-hydroxycoumarins, i.e., the parent compound of most derivatives listed in Tables 1 and 4, were synthesized according to classical procedures. *m*-Resorcinol (20 mmol) and the ethyl ester of an appropriate β -keto acid (22 mmol) were mixed and kept at 120 °C for 2 h with a catalytic amount of 96% sulfuric acid. After cooling to room temperature, the mixture was diluted with ethyl acetate and the solid filtered and purified by crystallization.

5,7-Dihydroxy-3,4-dimethylcoumarin. Yield: 43%; mp 294–6 °C dec, from ethyl acetate; ¹H NMR (CDCl₃ + 10% DMSO-*d*₆) δ 9.41 (s, 1 H, exch.), 9.28 (br, 1 H, exch.), 6.14 (d, 1 H, $J = 2.6$), 6.12 (d, 1 H, $J = 2.6$), 2.41 (s, 3 H), 1.92 (s, 3 H); IR (cm⁻¹) 3257, 1626, 1155. Anal. (C₁₁H₁₀O₄) C, H.

6,7-Dihydroxy-3,4-dimethylcoumarin was synthesized according to the procedure described by Tamura et al.⁴²

7-Amino-3,4-dimethylcoumarin. The parent compound of derivatives **16**, **23** and **28** was prepared by addition of ethyl 2-methylacetoacetate (1.4 g, 10 mmol) to a solution of 3-aminophenol (1.1 g, 10 mmol) in dry ethanol (50 mL). Zinc chloride (1.5 g) was then added and the reaction mixture heated for 30 min at reflux. Solvent was evaporated under reduced pressure and the obtained residue diluted in 50 mL of a 1:1 solution of chloroform and dioxane. The organic layer was extracted with 1 N NaOH, washed with brine, dried over Na₂SO₄ and concentrated in vacuum to give the desired compound in about 30% yield (lit.⁴³ 46% yield).

7-(Bromomethyl)coumarin. 7-Methylcoumarin (1.0 g, 6.2 mmol) was heated in refluxing carbon tetrachloride (20 mL). *N*-Bromosuccinimide (1.3 g, 7.5 mmol) and a catalytic amount of *N,N*-azobis(isobutyronitrile) (20 mg) were then added followed by 30 min of stirring. To the reaction mixture 20 mL of chloroform were added, and the organic layer was extracted with brine, dried over Na₂SO₄ and then concentrated under vacuum to give the desired compound in 69% yield: mp 164–5 °C, from EtOH; ¹H NMR (CDCl₃) δ 7.67 (d, 1 H, $J = 9.5$), 7.45

(d, 1 H, $J = 7.9$), 7.33 (d, 1 H, $J = 1.6$), 7.29 (dd, 1 H, $J = 7.9$, 1.6), 6.41 (d, 1 H, $J = 9.5$), 4.50 (s, 2 H); IR (cm⁻¹) 1724. Anal. (C₁₀H₇BrO₂) C, H.

General Procedure for the Alkylation of Hydroxy- or Aminocoumarins. Hydroxy or amino derivative of coumarin (10 mmol) was refluxed under magnetic stirring in 100 mL of absolute ethyl alcohol with 10 mmol of anhydrous potassium carbonate and 20 mmol of the suitable bromo derivative, until the reaction was complete (usually 1–4 h). The warm solution was filtered and cooled to room temperature to give a precipitate that was purified by crystallization. Through this procedure, compounds **3** and **4** were prepared by reacting 7-(bromomethyl)coumarin and phenol and aniline, respectively. Compound **16** was synthesized starting from 7-amino-3,4-dimethylcoumarin and benzyl bromide, whereas all the other derivatives in Tables 1 and 4 were obtained from the reaction of the appropriate hydroxycoumarin and benzyl or phenethyl (**17** and **18**) bromides.

3-(Benzyloxy)-6H-benzo[c]chromen-6-one (21). 2,3-Dichloro-5,6-dicyano-1,4-benzoquinone (DDQ) (0.23 g, 1.0 mmol) was added to a solution of **20** (0.31 g, 1.0 mmol), prepared according to patent literature,^{17,18} in anhydrous dioxane (10 mL). The reaction mixture was stirred for 2.5 h at reflux, then filtered off, concentrated under vacuum, and finally diluted with ethyl acetate. The organic layer was extracted with 2 N NaOH, washed with brine, dried over Na₂SO₄, and evaporated to dryness. The crude residue was purified by flash chromatography (CH₂Cl₂/hexane, 8:2 v/v, as the mobile phase), giving the pure product **21**.

N-(3,4-Dimethyl-2-oxo-2H-chromen-7-yl)benzamide (23). Benzoyl chloride (0.62 mL, 5.3 mmol) was added dropwise to a solution of 7-amino-3,4-dimethylcoumarin (1.01 g, 5.3 mmol) in 5 mL of 2 N NaOH, cooled at 0 °C. The reaction mixture was stirred for 15 min, and the white solid obtained filtered off and purified by crystallization.

N-(3,4-Dimethyl-2-oxo-2H-chromen-7-yl)-4-toluene-sulfonamide (28). An excess of 4-toluenesulfonyl chloride (0.57 g, 3.0 mmol) was added to a solution of 7-amino-3,4-dimethylcoumarin (0.19 g, 1.0 mmol) in 10 mL of anhydrous pyridine, cooled at 0 °C. The reaction mixture was stirred for 1 h, and then poured on ice, giving a precipitate that was filtered, washed, and purified by crystallization.

3,4-Dimethyl-7-[(E)-2-phenylethyl]-2H-chromen-2-one (29). 3-Styrylphenol was prepared via a Wittig reaction from 3-hydroxybenzaldehyde and benzyl triphenylphosphonium chloride in ethanolic solution of sodium ethylate, following the method described by Friedrich and Henning;²¹ both isomers (*trans* 60% and *cis* 40%) were obtained and separated by column chromatography using hexane/ethyl acetate (77.5:22.5 v/v) as eluent. Reaction of the *trans*-isomer²² with ethyl 2-methylacetoacetate, according to the above-reported general procedure for the synthesis of coumarin derivatives, yielded compound **29**.

7-(Benzyloxy)-6-hydroxy-3,4-dimethyl-2H-chromen-2-one (30), 6-(Benzyloxy)-7-hydroxy-3,4-dimethyl-2H-chromen-2-one (31), and 6,7-Bis(benzyloxy)-3,4-dimethyl-2H-chromen-2-one (32). These were prepared following the general procedure for the alkylation of coumarins bearing hydroxy groups, by reacting 6,7-dihydroxycoumarin (0.21 g, 1.0 mmol) with benzyl bromide (0.14 mL, 1.2 mmol). After evaporation of the solvent, the crude residue was washed with 5 mL of hot water, and the precipitate filtered off and separated by column chromatography using chloroform/hexane/ethyl acetate (90:5:5 v/v) as the mobile phase. The three compounds were well separated and their structures assessed by NOESY-NMR experiments.

5-(Benzyloxy)-7-hydroxy-3,4-dimethyl-2H-chromen-2-one (34). A solution of benzyl bromide (0.06 mL, 0.5 mmol) in 1 mL of absolute EtOH was added dropwise to a solution of 5,7-dihydroxy-3,4-dimethylcoumarin (0.21 g, 1.0 mmol) in 15 mL of absolute EtOH over a 4-h period, to minimize the formation of the dibenzyl derivative. After the usual workup, the residue was separated by column chromatography using

chloroform/ethyl acetate (80:20 v/v) as the mobile phase, and compound **34**, whose structure was assessed by a NOESY–NMR experiment, was obtained in 17% yield.

7-[(3-Hydroxybenzyl)oxy]-3,4-dimethyl-2H-chromen-2-one (52). *m*-Cresol was benzoyleated by a procedure similar to that described for compound **23**. 3-Methylphenyl benzoate, obtained as a white solid (42% yield), was brominated with NBS in CCl₄, according to the method described above for the preparation of 7-(bromomethyl)coumarin, to give α -bromo-3-methylphenyl benzoate (60% yield). This bromo derivative reacted with 7-hydroxy-3,4-dimethylcoumarin in the usual alkylation conditions to give **52**, which crystallized directly from the reaction mixture.

7-[(3-Aminobenzyl)oxy]-3,4-dimethyl-2H-chromen-2-one (55). Powdered zinc (0.22 g) was added to a hot solution of **61** (0.15 g, 0.34 mmol) in 17 mL of ethyl alcohol, under vigorous magnetic stirring, followed by dropwise addition of concentrated HCl (0.5 mL). The mixture was refluxed for 30 min, then cooled, filtered off, diluted with water and neutralized with 1 N NaOH. Compound **55** was obtained as a brown solid, by extraction with ethyl acetate and evaporation of the organic extracts to dryness.

N-(3-[(3,4-Dimethyl-2-oxo-2H-chromen-7-yl)oxy]-methyl)phenyl)acetamide (56). By treating **55** (0.65 g, 0.22 mmol) with acetic anhydride (1.0 mL) for 1 h at 0 °C, compound **56** was obtained after evaporation of the reaction mixture to dryness.

7-[(4-Fluoro-3-hydroxybenzyl)oxy]-3,4-dimethyl-2H-chromen-2-one (69). 2-Fluoro-5-methylphenol was treated with benzoyl chloride in the same conditions as for compound **23** (see above). The resulting 3-benzoyloxy-4-fluorotoluene (nearly quantitative yield) was brominated with NBS in CCl₄ (see above) to afford α -bromo-3-benzoyloxy-4-fluorotoluene (56% yield), which was used without further purification for the reaction with 7-hydroxy-3,4-dimethylcoumarin. The two compounds (1 mmol each) reacted for 8 h in 10 mL of refluxing anhydrous acetone, in the presence of 0.5 mmol of anhydrous K₂CO₃, to give 7-(3-benzoyloxy-4-fluorobenzoyloxy)-3,4-dimethyl-2H-chromen-2-one (39% yield) which was finally hydrolyzed with 2 equiv of NaOH in 10 mL of a mixture of EtOH/water (1:1, v/v) kept at 60 °C in an oil bath. The clear solution obtained was then concentrated under vacuum, acidified and extracted with ethyl acetate; the organic layers, dried over Na₂SO₄, were evaporated giving compound **69** as a solid.

The other newly synthesized coumarin derivatives (i.e., **3–6**, **8**, **13**, **54**, **70**, **71** in Tables 1 and 4) were prepared according to the literature as shown in general Scheme 1; their physicochemical and spectral data are listed in Table S1 (Supporting Information).

6-Benzoyloxy-4H-1-benzopyran-4-one (**36**) and its 2-methyl congener (**37**) were prepared by benzylation under classical conditions (see above for the general procedure) of the corresponding hydroxy derivatives, the latter being synthesized according to the methods described by Jaen et al.²⁷ and Pandit et al.,²⁸ respectively. Compounds **35**,⁴⁴ **38**⁴⁵ and **39**,⁴⁶ already known, were prepared following reported procedures.

The parent hydroxy compounds of the derivatives reported in Table 3, when not commercially available, were prepared using approaches already reported in the literature. Thus, 6-benzoyloxybenzofuran **42** was prepared according to a procedure described by Davies et al.,⁴⁷ whereas compound **41** was obtained by catalytic hydrogenation at 60 atm of **42**. Compounds **43**⁴⁸ and **45**⁴⁹ were prepared through benzylation of the hydroxy intermediates, synthesized according to known methods. 5-Hydroxyphthalimide,³⁰ the precursor of compound **46**, was prepared by reduction of *m*-nitrophthalimide with SnCl₂ in aqueous HCl, whereas diazotization/hydroxylation was achieved via a Sandmeyer reaction (35% yield).³¹

The starting material for the preparation of compound **48** was obtained from the reaction of 3-aminophenol with ethyl 2-methylacetoacetate under von Pechmann conditions (see above), whereas compound **47** was prepared using the approach of Teshima et al.⁵⁰

Physicochemical and spectral data of the newly synthesized chromones **36** and **37** and hetero-benzofused derivatives **43**, **44**, **46**, and **48** are reported in Table S1 (Supporting Information).

Biological Assays. Seventy-one compounds were tested for their inhibitory activity on MAO-A and MAO-B. Incubations were carried out at pH 7.4 (Na₂HPO₄/KH₂PO₄ made isotonic with KCl), 37 °C, in rat brain mitochondrial suspensions.⁵¹ A continuous spectrophotometric assay monitoring the rate of oxidation of the nonselective MAO substrate kynuramine into 4-hydroxyquinoline was used. Clorgyline (250 nM) or selegiline (250 nM) was preincubated with the suspension for 5 min to measure MAO-B or MAO-A activity, respectively. The formation of 4-hydroxyquinoline was followed at 314 nm using a Kontron UVIKON 941 spectrophotometer. The limited solubility of the tested compounds in aqueous solution required the use of 5% DMSO as cosolvent, a concentration that did not affect MAO activity. The substrate concentration used for the assays was 60 μ M for MAO-B and 90 μ M for MAO-A, corresponding to the respective *K_M* of kynuramine for the two isoenzymes. IC₅₀ values were determined and calculated from a hyperbolic equation as already described.⁵² Lineweaver–Burk plots on MAO-A and MAO-B were obtained from incubations at five substrate concentrations, without or with two different inhibitor concentrations. The inverse values of the reaction velocities were then represented as a function of the inverse value of substrate concentration.

p*K_a* Determination. A spectrophotometric method, as previously described,⁵³ was used for the determination of the p*K_a* of compound **28**. The spectra of the ionized and un-ionized forms were recorded in 0.1 M HCl and 0.1 M NaOH with 5% DMSO. A wavelength was chosen where the difference in absorbance between the un-ionized and ionized forms was maximal (λ = 347 nm). The absorbance values at 347 nm and different pH (7.4, 7.6, 7.0 and 6.8) were measured in a phosphate buffer (Na₂HPO₄/KH₂PO₄, 0.15 M) with 5% DMSO. The mean value was then determined and the standard deviation calculated (*n* = 4). The spectra and absorbance values were recorded on a Kontron UVIKON 941 spectrophotometer.

CoMFA (3D-QSAR) Study. All calculations were run on a workstation Silicon Graphics Indy R4400 175 MHz or Origin 2000 R10000 195 MHz using the SYBYL 6.6 molecular modeling package (Tripos Associates, St. Louis, MO). Minimal energy conformations were obtained using the MMFF94s force field.⁵⁴ Molecular electrostatic potential (MEP) was calculated with Gaussian 98 software⁵⁵ using the 3-21G* basis set. As a third field, the molecular lipophilicity potential (MLP) was used.⁵⁶ Statistics were performed with the QSAR module of SYBYL. Default settings were used except for the option “drop electrostatic”, which was set to “No”, meaning that the electrostatic field was calculated at grid points with high steric interactions ($\Delta 30$ kcal/mol). The GOLPE 4.5 software⁵⁷ (Multivariate Infometric Analysis, Perugia, Italy) was used to examine CoMFA statistical treatments and to validate and interpret the models. An advanced pretreatment was performed on the two data sets (A1 for MAO-A and B1 for MAO-B) for each field: steric (ste), electrostatic (mep), and lipophilic (lip). In both cases, “zeroing” positive and negative values was applied (ste: +0.5/–0.1; mep: +0.5/–0.1; lip: +0.2/–0.1 kcal/mol), as well as a standard deviation cutoff (ste: 0.1; mep: 1.0; lip: 0.1 kcal/mol). The 2-, 3- and 4-level variables were removed; for MAO-B inhibitors, the weights were set in order to give the same importance to each field. A grouping of variables was then applied using the smart region definition (SRD) algorithm: 163 seeds selected on PLS weights space, critical distance cutoff of 1.0 Å, and collapsing distance cutoff of 2.0 Å. The regions defined were then used in the fractional factorial design (FFD), which was finally applied to select the variables: a 5:1 ratio of true/dummy variables and a 2:1 ratio of combinations/variables were adopted. The cross-validation mode chosen was “leave-one-out” and the weights were recalculated after object exclusion. Noise variables were excluded and the uncertain ones were retained.

Acknowledgment. B.T. and P.A.C. are grateful to the Swiss National Science Foundation for financial support. A.C. and C.A. gratefully acknowledge the financial support of the National Council of Research (CNR-Rome, Italy).

Supporting Information Available: Table S1 giving all further information concerning the spectroscopic and physicochemical data of the newly synthesized compounds. This material is available free of charge via the Internet at <http://pubs.acs.org>.

References

- Bach, A. W. J.; Lan, N. C.; Johnson, D. L.; Abell, C. W.; Bembek, M. E.; Kwan, S. W.; Seeburg, P. H.; Shih, J. C. cDNA cloning of human liver monoamine oxidase A and B: molecular basis of differences in enzymatic properties. *Proc. Natl. Acad. Sci. U.S.A.* **1988**, *85*, 4934–4938.
- Grimsby, J.; Lan, N. C.; Neve, R.; Chen, K.; Shih, J. C. Tissue distribution of human monoamine oxidase A and B mRNA. *J. Neurochem.* **1990**, *55*, 1166–1169.
- Agid, Y.; Ahlskog, E.; Albanese, A.; Calne, D.; Chase, T.; De Yebenes, J.; Factor, S.; Fahn, S.; Gershnik, O.; Goetz, C.; Koller, W.; Kurth, M.; Lang, A.; Lees, A.; Lewitt, P.; Marsden, C. D.; Melamed, E.; Michel, P. P.; Mizuno, Y.; Obeso, J.; Oertel, W.; Olanow, W.; Poewe, W.; Pollak, K.; Tolosa, E. L-Dopa in the treatment of Parkinson's disease: a consensus meeting. *Movement Disorders* **1999**, *14*, 911–913.
- LeWitt, P. A. New drugs for the treatment of Parkinson's disease. *Pharmacotherapy* **2000**, *20*, 26S–32S.
- Drucharch, B.; van Muiswinkel, F. L. Drug treatment of Parkinson's disease. *Biochem. Pharmacol.* **2000**, *59*, 1023–1031.
- Walkinshaw, G.; Waters, C. M. Induction of apoptosis in catecholaminergic PC12 cells by L-dopa. Implications for the treatment of Parkinson's disease. *J. Clin. Invest.* **1995**, *95*, 2458–2464.
- Malorni, W.; Giammorioli, A. M.; Matarrese, P.; Pietrangeli, P.; Agostinelli, E.; Ciaccio, A.; Grassili, E.; Mondovi, B. Protection against apoptosis by monoamine oxidase A inhibitors. *FEBS Lett.* **1998**, *426*, 155–159.
- Harfenist, M.; Heuser, D. J.; Joyner, C. T.; Batchelor, J. F.; White, H. L. Selective inhibitors of monoamine oxidase. 3. Structure–activity relationship of tricyclic bearing imidazole, oxadiazole, or tetrazole groups. *J. Med. Chem.* **1996**, *39*, 1857–1863.
- Forna, L. S. Neuropathology of Parkinson's disease. *J. Neuro-pathol. Exp. Neurol.* **1996**, *55*, 259–272.
- Wouters, J. Structural aspects of monoamine oxidase and its reversible inhibition. *Curr. Med. Chem.* **1998**, *5*, 137–162.
- Kalgutkar, A. S.; Castagnoli, N., Jr.; Testa, B. Selective inhibitors of monoamine oxidase (MAO-A and MAO-B) as probes of its catalytic site and mechanism. *Med. Res. Rev.* **1995**, *15*, 325–388.
- Efange, S. M. N.; Boudreau, R. J. Molecular determinants in the bioactivation of the dopaminergic neurotoxin N-methyl-4-phenyl-1,2,3,6-tetrahydropyridine (MPTP). *J. Comput.-Aided Mol. Des.* **1991**, *5*, 405–417.
- Mabic, S.; Castagnoli, N., Jr. Assessment of structural requirements for the monoamine oxidase-B-catalyzed oxidation of 1,4-disubstituted-1,2,3,6-tetrahydropyridine derivatives related to the neurotoxin 1-methyl-4-phenyl-1,2,3,6-tetrahydropyridine. *J. Med. Chem.* **1996**, *39*, 3694–3700.
- Hoult, J. R. S.; Payd, M. Pharmacological and biochemical actions of simple coumarins: natural products with therapeutic potential. *Gen. Pharmacol.* **1996**, *27*, 713–722.
- Hossain, C. F.; Okuyama, E.; Yamazaki, M. A new series of coumarin derivatives having monoamine oxidase inhibitory activity from *Monascus anka*. *Chem. Pharm. Bull.* **1996**, *44*, 1535–1539.
- Rendenbach-Müller, B.; Schlecker, R.; Traut, M.; Weifenbach, H. Synthesis of coumarins as subtype-selective inhibitors of monoamine oxidase. *Bioorg. Med. Chem. Lett.* **1994**, *4*, 1195–1198.
- Rendenbach, B.; Weifenbach, H.; Teschendorf, H. J. Arylalkoxycoumarins. Verfahren zu ihre Herstellung und diese enthaltende therapeutische Mittel. Patent DE 3834861 A1, 1990 (BASF AG).
- Schlecker, R.; Schmidt, P.; Thieme, P. C.; Lenke, D.; Teschendorf, H. J.; Traut, M.; Mueller, C. D.; Hofmann, J. P.; Kreiskott, H. Neue Sulfonsäureester von Hydroxycoumarinen, ihre Herstellung und sie enthaltende Arzneimittel. Patent DE 3243158 A1, 1984 (BASF AG).
- van Pechmann, H. Duisberg, C. Über die verbindungen der Phenole mit Acetessigäther. *Chem. Ber.* **1883**, *16*, 2119–2128.
- Sethna, S.; Phadke, R. The Pechmann reaction. *Org. React.* **1953**, *7*, 1–58.
- Friedrich, K.; Henning, H. G. Darstellung stilbenartiger Verbindungen nach der Methode von G. Wittig. *Chem. Ber.* **1959**, *92*, 2944–2949.
- Bruce, J. M.; Creed, D.; Dawes, K. Light-induced and related reactions of quinones. Part VIII. Some (2-hydroxyalkyl)-, phenethyl-, (2-ethoxycarbonyl-ethyl)-, and styryl-1,4-benzoquinones. *J. Chem. Soc. C* **1971**, 3749–3753.
- Hoefnagel, A. J.; Gunnewegh, E. A.; Downing, R. S.; van Bekkum, H. Synthesis of 7-hydroxycoumarins catalysed by solid acid catalysts. *J. Chem. Soc., Chem. Commun.* **1995**, 225–226.
- Hermanson, M. A.; Barker, W. M.; Link, K. P. Studies on the 4-hydroxycoumarins. Synthesis, of the metabolites and some other derivatives of warfarin. *J. Med. Chem.* **1971**, *14*, 167–169.
- Dickenson, H. G. Cyclic lactones. U.S. Patent 2, 449, 162, Sept. 14, 1948; *Chem. Abstr.* **1949**, *43*, 694.
- Tamura, S.; Okuma, K.; Hayashi, T. The antioxygenic property of hydroxycoumarins. *J. Agric. Chem. Soc. Jpn.* **1952**, *26*, 413–414.
- Jaen, J. C.; Wise, L. D.; Heffner, T. G.; Pugsley, T. A.; Meltzer, L. T. Dopamine autoreceptor agonists as potential antipsychotics. 2. (Aminoalkoxy)-4H-1-benzopyran-4-ones. *J. Med. Chem.* **1991**, *34*, 248–256.
- Pandit, S. S.; Sethna, S. Molecular rearrangement of some o-acyloxyacylactones in the presence of metallic sodium. *J. Indian Chem. Soc.* **1950**, *27*, 1–4.
- Shigematsu, N. Synthetic analgesics. XVI. Synthesis of 1-(2-tertiary aminoalkyl)-3,4-dihydrocarbostyrils. *Chem. Pharm. Bull.* **1961**, *9*, 970–975.
- Wyrick, S. D.; Smith, F. T.; Kemp, W. E.; Grippo, A. A. Effects of [(N-alkyl-1,3-dioxo-1H,3H-isoindolin-5-yl)oxy]alkanoic acids, [(N-alkyl-1-oxo-1H,3H-isoindolin-5-yl)oxy]butanoic acids, and related derivatives on chloride influx in primary astroglial cultures. *J. Med. Chem.* **1987**, *30*, 1798–1806.
- Cohen, T.; Dietz, A. G., Jr.; Miser, J. R. A simple preparation of phenols from diazonium ions via the generation and oxidation of aryl radicals by copper salts. *J. Org. Chem.* **1977**, *42*, 2053–2058.
- MacLogP2.0; Biobyte Corp.: Claremont, CA, 1998.
- Hansch, C.; Leo, A. *Substituent Constants for Correlation Analysis in Chemistry and Biology*; John Wiley and Sons: New York, 1979; pp 352–352.
- Hansch, C.; Leo, A. *Exploring QSAR. Fundamentals and Applications in Chemistry and Biology*; ACS Professional Reference Book; American Chemical Society: Washington, DC, 1995; pp 1–557.
- van de Waterbeemd, H.; Testa, B. The parametrization of lipophilicity and other structural properties in drug design. In *Advances in Drug Research*; Testa, B., Ed.; Academic Press: London, 1987; Vol. 16, pp 87–227.
- Williams, S. G.; Norrington, F. E. Determination of positional weighting factors for the Swain and Lupton substituent constants F and R. *J. Am. Chem. Soc.* **1976**, *98*, 508–516.
- Kneubühler, S.; Thull, U.; Altomare, C.; Carta, V.; Gaillard, P.; Carrupt, P. A.; Carotti, A.; Testa, B. Inhibition of monoamine oxidase-B by 5H-indeno[1,2-c]pyridazine derivatives: biological activities, quantitative structure–activity relationships (QSARs) and 3D-QSARs. *J. Med. Chem.* **1995**, *38*, 3874–3883.
- Altomare, C.; Cellamare, S.; Summo, L.; Catto, M.; Carotti, A.; Thull, U.; Carrupt, P. A.; Testa, B.; Stoekli-Evans, H. Inhibition of monoamine oxidase-B by condensed pyridazines and pyrimidines: effects of lipophilicity and structure–activity relationships. *J. Med. Chem.* **1998**, *41*, 3812–3820.
- Cramer, R.D., III; Patterson, D. E.; Bunce, J. D. Comparative molecular field analysis (CoMFA). 1. Effect of shape on binding of steroids to carrier proteins. *J. Am. Chem. Soc.* **1988**, *110*, 5959–5967.
- Kaliszan, R.; Kaliszan, A.; Wainer, I. W. Deactivated hydrocarbonaceous silica and immobilized artificial membrane stationary phases in high-performance liquid chromatographic determination of hydrophobicities of organic bases: relationship to log P and CLOGP. *J. Pharm. Biomed. Anal.* **1993**, *11*, 505–511.
- Kim, K. H. Comparison of classical and 3D QSAR. In *3D QSAR in Drug Design. Theory Methods and Applications*; Kubinyi, H., Ed.; ESCOM Science Publishers: Leiden, 1993; pp 619–642.
- Pace, C. N.; Heinemann, U.; Hahn, U.; Saenger, W. Ribonuclease T1: structure, function, and stability. *Angew. Chem., Int. Ed. Engl.* **1991**, *30*, 343–360.
- Atkins, R. L.; Bliss, D. E. Substituted coumarins and azacoumarins. Synthesis and fluorescent properties. *J. Org. Chem.* **1978**, *43*, 1975–1980.
- Antus, S.; Gottsegen, A.; Nogradi, M. Unusual regioselectivity in the reduction of α,β -unsaturated carbonyl compounds with diisobutylaluminum hydride (DIBAL): direct conversion of isoflavones to iso-flavan-4-ones. *Synthesis* **1981**, *7*, 574–576.

- (45) Mahal, H. S.; Rai, H. S.; Venkataraman, K. Synthetical experiments in the chromone group. Part XVI. Chalcones and flavanones and their oxidation to flavones by means of selenium dioxide. *J. Chem. Soc.* **1935**, 866–868.
- (46) Bhalla, D. C.; Mahal, H. S. Synthetical experiments in the chromone group. Part XVII. Further observations on the action of sodamide on o-acyloxyacetophenones. *J. Chem. Soc.* **1935**, 868–870.
- (47) Davies, J. S. H.; McCrea, P. A.; Norris, W. L.; Ramage, G. L. Furanochromones. Part IV. Synthesis of 2-(methylfuran)-3',2'-(6,7)-chromone and derivatives thereof. *J. Chem. Soc.* **1950**, 3206–3213.
- (48) Vaughan, W. R.; Baird, S. L., Jr. The preparation of some phthalazines and related substances. *J. Am. Chem. Soc.* **1946**, 68, 1314–1316.
- (49) Beroza, M. 3,4-Methylenedioxyphenoxy compounds as synergists for natural and synthetic pyrethrins. *J. Agric. Food Chem.* **1956**, 4, 49–53.
- (50) Teshima, T.; Nakaji, A.; Shiba, T.; Tsai, L.; Yamazaki, S. Elucidation of stereospecificity of a selenium-containing hydrogenase from *Metanococcus Vannielii*. Synthesis of (R)- and (S)-[4-²H₁]-3,4-dihydro-7-hydroxy-1-hydroxyethylquinolinone. *Tetrahedron Lett.* **1998**, 26, 351–354.
- (51) Thull, U.; Kneubühler, S.; Gaillard, P.; Carrupt, P. A.; Testa, B.; Altomare, C.; Carotti, A.; Jenner, P.; McNaught, K. S. P. Inhibition of monoamine oxidase by isoquinoline derivatives: qualitative and 3D-quantitative structure–activity relationships. *Biochem. Pharmacol.* **1995**, 50, 869–877.
- (52) Thull, U.; Kneubühler, S.; Testa, B.; Borges, M. F. M.; Pinto, M. M. M. Substituted xanthenes as selective and reversible monoamine oxidase A (MAO-A) inhibitors. *Pharm. Res.* **1993**, 10, 1187–1190.
- (53) Albert, A.; Serjeant, E. P. Determination of ionization constants by spectrophotometry. *The Determination of Ionization Constants. A Laboratory Manual*; Chapman and Hall: London, 1984; pp 70–95.
- (54) Halgren, T. A. Merck molecular force field. II. MMFF94 van der Waals and electrostatic parameters for intermolecular interactions. *J. Comput. Chem.* **1996**, 17, 520–552.
- (55) Frish, M. J.; Trucks, G. W.; Schlegel, H. B.; Scuseria, M. A.; Robb, M. A.; Cheeseman, J. R.; Zahrzewski, V. G.; Montgomery, J. A.; Stratmann, R. E.; Burant, J. C.; Dapprich, S.; Millam, J. M.; Daniels, A. D.; Kudin, K. N.; Strain, M. C.; Farkas, O.; Tomasi, J.; Barone, V.; Cossi, M.; Cammi, R.; Mennucci, B.; Pomelli, C.; Adamo, C.; Clifford, S.; Ochterski, J.; Petersson, G. A.; Ayala, P. Y.; Cui, Q.; Morokuma, K.; Malick, D. K.; Rabuck, A. D.; Raghavachari, K.; Foresman, J. B.; Cioslowski, J.; Ortiz, J. V.; Stefanov, B. B.; Liu, G.; Liashenko, A.; Piskorz, P.; Komaromi, I.; Gomperts, R.; Martin, R. L.; Fox, D. J.; Keith, T.; Al-Laham, M. A.; Peng, C. Y.; Nanayakkara, A.; Gonzalez, C.; Challacombe, M.; Gill, P. M. W.; Johnson, B. G.; Chen, W.; Wong, M. W.; Andres, J. L.; Head-Gordon, M.; Replogle, E. S.; Pople, J. A. *GAUSSIAN 98 software*, revision A.1; Gaussian, Inc.: Pittsburgh, PA, 1998.
- (56) Gaillard, P.; Carrupt, P. A.; Testa, B.; Boudon, A. Molecular lipophilicity potential, a tool in 3D-QSAR. Method and applications. *J. Comput.-Aided Mol. Des.* **1994**, 8, 83–96.
- (57) *GOLPE 4.5*; Multivariate Infometric Analysis: Perugia, Italy, 1999.

JM001028O